

This discussion paper is/has been under review for the journal Atmospheric Chemistry and Physics (ACP). Please refer to the corresponding final paper in ACP if available.

**Bromocarbon
oceanic emissions
and upper air
concentrations**

S. Tegtmeier et al.

Bridging the gap between bromocarbon oceanic emissions and upper air concentrations

S. Tegtmeier¹, K. Krüger¹, B. Quack¹, I. Pisso², A. Stohl³, and X. Yang^{4,5}

¹IFM-GEOMAR, Kiel, Germany

²Research Institute for Global Change, JAMSTEC, Yokohama, Japan

³Norwegian Institute for Air Research (NILU), Kjeller, Norway

⁴National Centre for Atmospheric Science (NCAS), Cambridge, UK

⁵University of Cambridge, Department of Chemistry, Cambridge, UK

Received: 12 January 2012 – Accepted: 14 January 2012 – Published: 8 February 2012

Correspondence to: S. Tegtmeier (stegtmeier@geomar.de)

Published by Copernicus Publications on behalf of the European Geosciences Union.

Title Page

Abstract

Introduction

Conclusions

References

Tables

Figures

⏪

⏩

◀

▶

Back

Close

Full Screen / Esc

Printer-friendly Version

Interactive Discussion

Abstract

Oceanic emissions of halogenated very short-lived substances (VSLS) are expected to contribute significantly to the stratospheric halogen loading and therefore to ozone depletion. Estimates of the amount of VSLS transported into the stratosphere are highly uncertain and based on sporadic observations around the tropical tropopause layer (TTL) and on modeling studies which use prescribed emission scenarios to reproduce observed atmospheric concentrations. Actual measurements of VSLS emissions at the ocean surface have not been linked to the stratospheric halogen loading until now. Here we use observations of oceanic VSLS emissions in the western Pacific and an atmospheric Lagrangian transport model to estimate the direct contribution of bromoform (CHBr_3), and dibromomethane (CH_2Br_2) to the stratospheric bromine loading. Our emission-based estimates of VSLS profiles provide the first link between observed oceanic emissions and in situ TTL measurements. The emission-based and observed profiles of CHBr_3 show good agreement, confirming the importance of the western Pacific as a source region. However, CH_2Br_2 emission-based estimates are considerable smaller than current upper air observations as a result of relatively low western Pacific emissions. We estimate the relative importance of the highly variable emission rates and the surface to stratosphere transport for the contribution of the two bromocarbons to the stratospheric bromine budget. Our results show that stratospheric entrainment of bromine in form of VSLS or their degradation products is highly variable and that this variability is primarily linked to the variability of the observed sea-to-air flux. Together, both bromocarbons contribute to the stratospheric bromine budget with 0.4 pptv on average and 2.3 pptv for cases of maximum emissions.

ACPD

12, 4477–4505, 2012

Bromocarbon oceanic emissions and upper air concentrations

S. Tegtmeier et al.

Title Page

Abstract

Introduction

Conclusions

References

Tables

Figures

⏪

⏩

◀

▶

Back

Close

Full Screen / Esc

Printer-friendly Version

Interactive Discussion

1 Introduction

Organic brominated compounds, emitted at the surface through natural and anthropogenic processes, are the primary source of stratospheric bromine. While brominated substances are transported through troposphere and stratosphere, inorganic bromine (Br_y) is released via photolysis or reaction with OH. Once released the reactive bromine species are known to participate in catalytic ozone destruction in the stratosphere (McElroy et al., 1986; Solomon et al., 1995; Garcia and Solomon, 1994) and may also have a significant impact on tropospheric ozone (von Glasow et al., 2004; Yang et al., 2005). However, the contributions of individual bromine sources to the stratospheric Br_y budget as well as the abundance of tropospheric bromine are still highly uncertain.

Long-lived bromocarbons with chemical lifetimes of years are well mixed in the troposphere and transported into the stratosphere without any significant chemical loss. In contrast, very short-lived substances (VSLs) have chemical lifetimes of less than 6 months (e.g., Ko and Poulet et al., 2003) and are often oxidized or photolyzed in the troposphere. In case the VSLs reach the stratosphere before being photochemically destroyed they provide an in-situ source of stratospheric Br_y upon their degradation. The cross-tropopause transport of VSLs is referred to as source gas injection (SGI). In case the VSLs are destroyed in the troposphere inorganic bromine is produced which is soluble and can be removed from the troposphere by wet deposition. If however, the inorganic product gases are transported into the stratosphere before being washed out, a process referred to as product gas injection (PGI), they will add to the stratospheric Br_y budget. The dehydration of air masses during troposphere-to-stratosphere transport is not completely understood so far and therefore estimates of the wet deposition of Br_y are highly uncertain (Montzka and Reimann et al., 2011). Overall, the rate of SGI and PGI depends strongly on the efficiency of troposphere-to-stratosphere transport compared to the degradation of source gases (through photochemical loss) and product gases (through wet deposition). As a result, estimating the contribution of

ACPD

12, 4477–4505, 2012

Bromocarbon oceanic emissions and upper air concentrations

S. Tegtmeier et al.

Title Page

Abstract

Introduction

Conclusions

References

Tables

Figures

⏪

⏩

◀

▶

Back

Close

Full Screen / Esc

Printer-friendly Version

Interactive Discussion

bromine containing VSLs to stratospheric Br_y is by far more complicated than doing so for the long-lived bromocarbons.

Measurements of VSLs are scarce and current estimates of their contribution to stratospheric Br_y range from 1.5 to 8 pptv based on balloon-borne measurements (Dorf et al., 2008), ground-based observations of column BrO (Sinnhuber et al., 2002, and references therein), and satellite BrO measurements (Sinnhuber et al., 2005; Livesey et al., 2006; Sioris et al., 2006; McLinden et al., 2010). In addition to the estimates based on in situ and satellite observations several recent modeling studies are available which focus on bromoform (CHBr_3) and dibromomethan (CH_2Br_2), the two most abundant short-lived bromocarbons (Law and Sturges et al., 2007). Their contribution to stratospheric Br_y is estimated to be $\sim 2\text{--}5$ pptv (Kerkweg et al., 2008; Gettelman et al., 2009; Aschmann et al., 2009; Hossaini et al., 2010; Liang et al., 2010) which is less than suggested by observations. A modeling study from Warwick et al. (2006) taking into account all five major short-lived bromocarbons yields estimates of 6–7 pptv. The model studies either used prescribed removal timescales for Br_y in the Tropical Tropopause Layer (TTL) or explicitly calculate the Br_y removal based on dehydration processes in the model. There are large differences in the effect of washout predicted by models which together with the lack of observations of bromine PG in the TTL result in a wide range of CHBr_3 and CH_2Br_2 PGI from 0.4 to 3.9 ppt. The upper limit of SGI and PGI estimates obtained from observations and models would imply a relatively large impact of stratospheric inorganic bromine produced from VSLs ($\text{Br}_y^{\text{VSLs}}$) on mid-latitude ozone depletion (Salawitch et al., 2005). Therefore the extent to which VSLs contribute to the stratospheric Br_y budget remains a key question of ongoing research.

CHBr_3 and CH_2Br_2 are expected to account for a large fraction of stratospheric $\text{Br}_y^{\text{VSLs}}$. The uncertainty in the contribution of the two VSLs to stratospheric Br_y originates partially from the uncertainty in the efficiency of SGI and PGI and partially from strongly variable sources. CHBr_3 is mainly produced in the ocean by marine life forms such as macro algae, ice algae and phytoplankton (e.g., Carpenter and Liss, 2000; Quack and Wallace, 2003), while CH_2Br_2 is a by-product during the CHBr_3 forma-

Bromocarbon oceanic emissions and upper air concentrations

S. Tegtmeier et al.

Title Page

Abstract

Introduction

Conclusions

References

Tables

Figures

⏪

⏩

◀

▶

Back

Close

Full Screen / Esc

Printer-friendly Version

Interactive Discussion



tion (Tokarczyk and Moore, 1994). The oceanic production and thereafter the ocean-to-atmosphere flux of CHBr_3 is spatially and temporal highly variable with tropical, subtropical and shelf waters being identified as potentially important source regions (Quack et al., 2004; Butler et al., 2007; Quack et al., 2007). Observational estimates of local oceanic emissions of the two VSLs are based on measurements of surface water and atmospheric concentration data. In general, only data of limited spatial and temporal coverage are available. As a result, current estimates of oceanic emissions of CHBr_3 and also of CH_2Br_2 are a major source of uncertainty in atmospheric modeling studies which often rely on uniformly mixed background mixing ratios and might miss the influence of strongly localized sources. This would be particularly problematic in case of a correlation between emission strength and efficiency of transport into the TTL, resulting in systematic over- or underestimates of PGI and SGI when using averaged emission fluxes. Due to the large regional differences in the CHBr_3 emission rates and its short tropospheric lifetime of 15–30 days (Hossaini et al., 2010) compared to atmospheric transport time scales the tropospheric CHBr_3 distribution is highly variable in time and space. CH_2Br_2 has a longer tropospheric lifetime (50–400 days) than CHBr_3 , however, not long enough to be well mixed in the troposphere. CHBr_3 and CH_2Br_2 measurements in the upper troposphere and TTL region are available from a few aircraft and balloon campaigns (Schauffler et al., 1998; Schauffler et al., 1999; Sinnhuber and Folkins, 2006; Law and Sturges et al., 2007; Laube et al., 2008) and show a large spread. A current challenge is to relate the variability of observed VSLs sea-to-air fluxes to the variability of measured VSLs in the upper troposphere and TTL region.

In this study we use sea-to-air fluxes of CHBr_3 and CH_2Br_2 obtained from ship-based measurements to estimate their SGI and PGI into the stratosphere. The measurements were done during the TransBrom Sonne cruise in the tropical western Pacific in 2009 as described in Sect. 2.1. The transport calculations are carried out with the Lagrangian particle dispersion model FLEXPART which is introduced in Sect. 2.2. Results of the transport calculations including estimates of the amount of VSLs and their degrada-

**Bromocarbon
oceanic emissions
and upper air
concentrations**

S. Tegtmeier et al.

Title Page

Abstract

Introduction

Conclusions

References

Tables

Figures



Back

Close

Full Screen / Esc

Printer-friendly Version

Interactive Discussion

tion products transported into the TTL are presented in Sect. 3. Simulated CHBr_3 and CH_2Br_2 vertical profiles are compared with aircraft observations. Analyzing how emission rates and convective activity influence SGI and PGI will help to understand the relative importance of these two processes for the stratospheric Br_y budget.

2 Data and model

2.1 Sonne TransBrom campaign

Atmospheric and oceanic CHBr_3 and CH_2Br_2 were measured during the TransBrom cruise with the R/V *Sonne* from Tomakomai, Japan, 9 October 2009 to Townsville, Australia, 23 October 2009 (Krüger and Quack, 2012). The time of the ship cruise was within the season of high typhoon occurrence in the tropical western Pacific, a region which is in general characterized by the globally highest convective activity (“warm pool”) throughout the year. The cruise track crossed the typhoon Melor in the northern extratropics and the two tropical depressions Nepartak and Lupit. The transit route from Japan to Australia followed almost exactly the 146° E meridian from 44° N to 18° S through extratropical and tropical regions. The TTL had a latitudinal extension from at least 36° N to 18° S during the time of the ship cruise.

Surface air samples were collected every 3 hours during the cruise section from 32.6° N to 18.7° S in pressurized stainless steel canisters. The air samples were analyzed subsequently for CHBr_3 , CH_2Br_2 and other VSLS at the Rosenstiel School of Marine and Atmospheric Sciences (RSMAS) in Miami by the group of Elliot Atlas following the method from Schauffler et al. (1999). Surface water samples were collected simultaneously by a submersible pump at 5m depth and analyzed on board using a purge-and-trap GC/MS analytical system. A detailed description of the system can be found in Quack et al. (2004). The instantaneous sea-to-air flux of CHBr_3 and CH_2Br_2 was calculated from the measured sea surface concentration and local atmospheric mixing ratios, Henry’s law constant from Moore et al. (2005) and the instantaneous

Bromocarbon oceanic emissions and upper air concentrations

S. Tegtmeier et al.

Title Page

Abstract

Introduction

Conclusions

References

Tables

Figures



Back

Close

Full Screen / Esc

Printer-friendly Version

Interactive Discussion

wind speed. The flux calculations are based on the transfer coefficient parameterization of Nightingale et al. (2000), which were adapted to CHBr_3 and CH_2Br_2 (Quack and Wallace, 2003).

2.2 FLEXPART trajectories

The atmospheric transport of CHBr_3 and CH_2Br_2 from the oceanic surface into the upper troposphere and TTL is simulated with the Lagrangian particle dispersion model FLEXPART (Stohl et al., 2005). This model has been used extensively in studies of long-range and mesoscale transport (e.g., Spichtinger et al., 2001; Stohl et al., 2003; Forster et al., 2004). Validation of FLEXPART is based on comparisons with measurement data from three large-scale tracer experiments (Stohl et al., 1998) and on inter-continental air pollution transport studies (e.g. Stohl and Trickl, 1999; Forster et al., 2001; Spichtinger et al., 2001). FLEXPART is an off-line model driven by meteorological fields from the ECMWF (European Centre for Medium-Range Weather Forecasts) numerical weather prediction model. It includes parameterizations for moist convection (Forster et al., 2007), turbulence in the boundary layer and free troposphere (Stohl and Thompson, 1999), dry deposition and in-cloud as well as below-cloud scavenging, and the simulation of chemical decay.

In order to describe the transport and dispersion of CHBr_3 , we simulate trajectories of a multitude of air parcels, each carrying a mass fraction of the VSL5 tracer. For each data point of the observed sea-to-air flux a separate FLEXPART run is launched where 10 000 air parcels were released over one hour from a $0.0002^\circ \times 0.0002^\circ$ grid box ($\sim 500 \text{ m}^2$) at the ocean surface centered at the measurement location. The total amount of CHBr_3 emitted from this grid box over one hour is calculated based on the observation-derived flux and uniformly distributed over the 10 000 air parcels. The FLEXPART runs are driven by the ECMWF reanalysis product ERA-Interim (Dee et al., 2011) given at a horizontal resolution of $1^\circ \times 1^\circ$ on 60 model levels. Transport, dispersion and convection of the air parcels are calculated from the 6-hourly fields of horizontal and vertical wind, temperature, specific humidity, convective and large

Bromocarbon oceanic emissions and upper air concentrations

S. Tegtmeier et al.

Title Page

Abstract

Introduction

Conclusions

References

Tables

Figures

⏪

⏩

◀

▶

Back

Close

Full Screen / Esc

Printer-friendly Version

Interactive Discussion



scale precipitation and others. The input data is retrieved from the ECMWF archives using a pre-processor which calculates the vertical wind in hybrid coordinates mass-consistently from spectral data.

Figure 1 illustrates a FLEXPART run for one case study based on the emitted CHBr_3 flux observed during the TransBrom Sonne campaign at 19°N , 148°E on 14 October 2009 at 11 a.m. UTC. The spatial distribution of all 10 000 air parcels on 24 October 2009, 10 days after their release from the measurement location, is displayed. A large fraction of the air parcels is spread out over the maritime continent, Southeast Asia, India, and the tropical Indian Ocean all the way from the west coast of Australia to the east coast of Africa. A smaller fraction of air parcels has been transported eastwards from the release location and is now distributed along two narrow latitude bands at roughly 30°N and 30°S across the tropical Pacific. Overall, a large number of air parcels have reached altitudes above 10 km which illustrates the strong impact of deep convection on the vertical transport observed for this case study. Each air parcel carries an assigned mass of the CHBr_3 tracer which is reduced at a rate corresponding to its chemical lifetime.

2.3 Wet deposition of Br_y

The degradation of CHBr_3 and CH_2Br_2 along each trajectory is simulated by prescribing an altitude dependent chemical lifetime, ranging from 16 (50) days at the ocean surface to 29 (400) days in the TTL for CHBr_3 (CH_2Br_2) (Hossaini et al., 2010). The fraction of photochemically destroyed CHBr_3 and CH_2Br_2 contributes to the inorganic product gases which are grouped together as Br_y and are transported together with the VLSL source gases along the trajectory. The assumption of instantaneous conversion between organic intermediate product gases and Br_y has been shown to be reasonable (Hossaini et al., 2010). Br_y can be removed from the troposphere by wet deposition which is initiated in FLEXPART if the relative humidity exceeds a certain threshold. The resultant washout is modeled via the cloud scavenging ratio calculated with the help of the effective Henry coefficient. Within the family of inorganic bromine, HOBr and

Bromocarbon oceanic emissions and upper air concentrations

S. Tegtmeier et al.

Title Page

Abstract

Introduction

Conclusions

References

Tables

Figures

⏪

⏩

◀

▶

Back

Close

Full Screen / Esc

Printer-friendly Version

Interactive Discussion



HBr can be washed out while the remaining species Br, BrO, BrONO₂, and Br₂ are not soluble. HOBr and HBr have different solubility properties which are described by different Henry coefficients. In order to determine which fractions of Br_y are in the form of HBr and HOBr and which fraction is not soluble we apply the Br_y partitioning modeled with the Chemical Transport Model (CTM) p-TOMCAT (Yang et al., 2010). The model uses analysed wind-fields together with complex chemical schemes to simulate the tracer distribution in the troposphere and lower stratosphere. The 3-dimensional Br_y field from p-TOMCAT and its partitioning into HOBr, HBr, Br, BrO, BrONO₂, and Br₂ are given every 30 min for October 2009. The partitioning of the Br_y field into the individual members of the Br_y family varies strongly with location and time and is applied to every air parcel according to its location each time before the wet deposition is initiated. Wet deposition is then calculated individually for each member of the Br_y family in order to realistically simulate the Br_y removal along the trajectories.

2.4 Ozone Depletion Potential

The Ozone Depletion Potential (ODP), a measure of a substance's destructive effects to the ozone layer relative to the reference substance CFC-11 (CCl₃F) is estimated for CHBr₃ and CH₂Br₂. The ODPs are determined by the fraction of VSLs which reach the stratosphere and their subsequent residence time in the stratosphere, during which ozone depletion can occur. The ODPs for CHBr₃ and CH₂Br₂ are calculated as a function of location and time of emission following a previously developed trajectory-based method (Pisso et al., 2010). Owing to the different timescales and processes in the troposphere and stratosphere, the estimates are based on separate ensembles of trajectories calculated for air masses emitted in the western Pacific in October 2009. The tropospheric trajectories are used to quantify the fraction of VSLs reaching the stratosphere while stratospheric trajectories are run for longer time periods in order to determine stratospheric residence time. Results from the two trajectory ensembles are combined in order to estimate the VSLs ODP as a function of emission location. Uncertainties of the method are associated with tropospheric chemistry and transport,

Bromocarbon oceanic emissions and upper air concentrations

S. Tegtmeier et al.

Title Page

Abstract

Introduction

Conclusions

References

Tables

Figures

⏪

⏩

◀

▶

Back

Close

Full Screen / Esc

Printer-friendly Version

Interactive Discussion



but also with the representation of stratospheric chemistry (ozone depletion by heterogeneous reactions) and transport (large scale circulation). A depletion efficiency factor of 60 is used for Br (Law and Sturges et al., 2007; Montzka and Reimann et al., 2011). The average stratospheric residence time for active chlorine is assumed to be 60 months.

2.5 VLSL vertical profiles

The VLSL vertical profiles represent the VLSL mixing ratios averaged over all air parcels which have been originally emitted at one measurement site above a certain atmospheric level. The profiles are estimated from the overall amount of VLSL entrained above an atmospheric level together with the overall amount of air entrained above this level. In order to account for the fact that our VLSL emission grid box is very small while the air entrained above a certain level originates from all over the globe we scale the amount of air so that it is proportional to the size and duration of the emission grid box. Note, that since we cannot account for mixing with air masses from other regions the profiles are not assumed to be real atmospheric profiles but rather display profiles one would expect if one would assume emission and atmospheric transport properties as observed in the western Pacific globally. In other words our estimated profiles describe the relative contribution of western Pacific emissions to atmospheric VLSL mixing ratios. Uncertainties in our estimates of VLSL abundance in the upper TTL are associated with uncertainties in the convective parameterization, the vertical transport driven by the vertical wind fields and the prescribed lifetime of the species. Testing the model sensitivity shows that our results are mainly constrained by the accurate representation of convection (which has been validated with tracer experiments and ^{222}Rn measurements in Forster et al., 2007), with small variations in the prescribed lifetime leading only to small differences in the derived VLSL profiles. Applying transport timescales based on vertical heating rates instead of vertical wind fields in the TTL between 15 and 17 km also results in only minor differences.

Bromocarbon oceanic emissions and upper air concentrations

S. Tegtmeier et al.

Title Page

Abstract

Introduction

Conclusions

References

Tables

Figures



Back

Close

Full Screen / Esc

Printer-friendly Version

Interactive Discussion



3 Results

3.1 Case study of CHBr_3 transport

Four case studies of modeled CHBr_3 transport which are characterized by highly variable emission and transport properties are analyzed. The first case study is based on an example of a relatively low CHBr_3 sea-to-air flux of $110.6 \text{ pmol m}^{-2} \text{ h}^{-1}$ observed at 30° N , 145° E on 10 October 2009. The black line in Fig. 2a shows the vertical distribution of CHBr_3 10 days after the release event which has been obtained by adding up the amount of trace gas contained in all tropical ($30^\circ \text{ N} - 30^\circ \text{ S}$) air parcels. The vertical distribution of CHBr_3 peaks between 2 and 8 km and only a very small fraction of the air masses has been transported into the TTL. Figure 2b shows the vertical distribution of CHBr_3 over a one month time period starting at the date of the release event on October 10. Most air masses remain in the region below 10 km over the entire month due to the lack of deep convection. The second case study, displayed in Fig. 2c, is based on the CHBr_3 sea-to-air flux observed at 19° N , 148° E on 14 October 2009 which was also very low with $133.4 \text{ pmol m}^{-2} \text{ h}^{-1}$. Air mass transport for this example has been discussed in the previous section including the presentation of the spatial distribution of all air parcels 10 days after the release. The slowly decreasing concentrations of CHBr_3 over time are caused by the chemical decay of the tracer. Also mixing into the extratropics will decrease the total amount of tropical CHBr_3 . However Fig. 1 indicated that this process is weak and most air masses remain between 30° N and 30° S . The total amount of CHBr_3 entrained above a certain level is calculated as the sum of CHBr_3 carried by all the trajectories which cross that level. For case study 2 the total amount of CHBr_3 entrained above 17 km is 5.9 nmol. Compared to case study 1 this example shows quite the opposite behavior with strong upward transport of CHBr_3 over a very short time period of only hours to days right after the release event which is evident from the tracer distribution. The strong convective activity lifting the majority of the air masses is very likely related to the tropical depression observed close to the measurement location.

Bromocarbon oceanic emissions and upper air concentrations

S. Tegtmeier et al.

[Title Page](#)[Abstract](#)[Introduction](#)[Conclusions](#)[References](#)[Tables](#)[Figures](#)[⏪](#)[⏩](#)[◀](#)[▶](#)[Back](#)[Close](#)[Full Screen / Esc](#)[Printer-friendly Version](#)[Interactive Discussion](#)

A direct comparison of the vertical distribution of CHBr_3 10 days after the release event between the two case studies can be seen in Fig. 2a illustrating the highly variable vertical distribution of CHBr_3 as a result of the impact of deep convection. Case study 3 is based on the sea-to-air flux observed at 3°S , 154°E on 19 October 2009, while case study 4 describes the flux observed at 18°S , 145°E on 23 October 2009. Both case studies are chosen since they describe so-called hot-spots of emissions with very high fluxes of 2875.71 and $4551.7 \text{ pmol m}^{-2} \text{ h}^{-1}$, respectively. The subsequent transport of the large amounts of CHBr_3 develops very differently for the two events with case study 3 displaying strong convective events influencing transport up to 14/15 km during the first 10 days (Fig. 2e), while case study 4 shows the strongest impact of convection below 10 km (Fig. 2f). A comparison 10 days after the release event reveals that for case study 4 most of the CHBr_3 is still between 0 and 3 km, while case study 3 results in most of the CHBr_3 between 9 and 15 km (Fig. 2d). The four case studies demonstrate that we find a high variability in emission strength and transport intensity which will be analyzed systematically in the following paragraph.

3.2 SGI and PGI during the Sonne-Transbrom cruise

Modeling of transport, chemical decay and wet deposition of CHBr_3 , CH_2Br_2 and Br_y as described in Sect. 2 has been carried out for all observations of sea-to-air fluxes obtained during the TransBrom Sonne campaign. For each of the 103 observed CHBr_3 and 64 CH_2Br_2 fluxes a FLEXPART simulation analogous to the examples illustrated above was performed. Figure 3a and b show the oceanic emission rates (black lines) of the two major bromocarbons as observed during the ship campaign in the western Pacific. The oceanic emissions of both trace gases are characterized by a strong variability along the cruise track, linked to wind speed variations and differences in the compounds saturation state. Currently available global estimates of oceanic emissions of CHBr_3 and CH_2Br_2 can differ approximately by a factor four and are highly uncertain (Montzka and Reimann et al., 2011). The mean emission rates observed in the western Pacific in October 2009 for CHBr_3 of $536.7 \text{ pmol m}^{-2} \text{ h}^{-1}$ are approximately in

Bromocarbon oceanic emissions and upper air concentrations

S. Tegtmeier et al.

Title Page

Abstract

Introduction

Conclusions

References

Tables

Figures

⏪

⏩

◀

▶

Back

Close

Full Screen / Esc

Printer-friendly Version

Interactive Discussion



the middle of the range of global mean values (Carpenter and Liss, 2000; Quack and Wallace, 2003), whereas the mean rates for CH_2Br_2 of $163.5 \text{ pmol m}^{-2} \text{ h}^{-1}$ are only slightly larger than the lowest global estimate (Yokouchi et al., 2005).

The cold point in the vertical temperature profile at around 17 km is of special importance for SGI and PGI. Above this level no significant washout is expected and VLSL product gases and source gases reaching this altitude can be assumed to contribute to the stratospheric halogen loading irrespective of their remaining chemical lifetime. The amount of VLSL product gases entrained above 17 km is calculated as the sum of CHBr_3 or CH_2Br_2 , respectively, carried by all the computational particles which cross this level. For each observed oceanic VLSL emission along the cruise track we determine the fraction of the originally emitted amount of CHBr_3 and CH_2Br_2 entrained above the 17 km surface. On average, these fractions range from 15 % for CH_2Br_2 to 4 % for CHBr_3 , indicating decreasing efficiency of vertical transport with decreasing lifetime. The time series of the entrained VLSL fractions as a function of latitude along the cruise track is displayed in Fig. 3a and b for CHBr_3 and CH_2Br_2 , respectively (colored dots). Rapid vertical uplift in deep convection provides the major pathway for VLSL from the surface to the TTL. The variability of convection occurrence has a stronger impact on the shorter lived gas CHBr_3 as evident from its highly variable entrained VLSL fractions. We find the largest CHBr_3 entrainment of up to 10 % during the first part of the cruise at around 20° N related to the strong vertical uplift observed during the developing typhoon Lupit (Krüger and Quack, 2011). During the second part of the cruise vertical transport is less intense and therefore the fractional entrainment is lower reaching values between 2 and 5 %. For CH_2Br_2 the fractional entrainment is overall larger and shows less variability compared to CHBr_3 as a result of the longer lifetime. Together, the VLSL emissions and the transport efficiency (expressed as the entrained VLSL fractions) determine the total amount of VLSL entrained above the 17 km surface (colored lines in Fig. 3a and b). The hot spot emissions during the second part of the cruise result in strongest VLSL entrainment although the vertical transport intensity is larger during the first part of the cruise. If events of strong vertical transport would coin-

Bromocarbon oceanic emissions and upper air concentrations

S. Tegtmeier et al.

Title Page

Abstract

Introduction

Conclusions

References

Tables

Figures

⏪

⏩

◀

▶

Back

Close

Full Screen / Esc

Printer-friendly Version

Interactive Discussion

cide with strong VSLs emissions one could expect very large amounts of VSLs being transported into the stratosphere. However, strong localized oceanic sources related to coastal regions determine the peak emissions and therefore no direct link between emission strength and wind variations or vertical transport intensity exists. For both bromocarbons the total entrainment is highly correlated with the surface emissions ($r > 0.95$) but not correlated with the transport efficiency.

The contribution of VSLs to the stratospheric bromine loading depends on SGI as discussed above and also on PGI where inorganic bromine resulting from the degradation of CHBr_3 and CH_2Br_2 is entrained into the stratosphere. Similar to what has been done for the VSLs source gases the Br_y entrainment above the cold point has been estimated. Considerably more Br_y originating from the degradation of CHBr_3 than from the degradation of CH_2Br_2 is entrained into the stratosphere (Fig. 3c). This is due to stronger CHBr_3 fluxes and the fact that CHBr_3 contains one more bromine atom than CH_2Br_2 . Additionally, for CH_2Br_2 a larger fraction is entrained already as source gas and therefore less bromine is left for potential product gases. Maximum amounts of PGs are transported into the stratosphere for peak emission events similar to what has been noted for the SGI. Overall SGI and PGI of bromocarbons emitted in the western Pacific are determined by the intensity of surface emissions and show the same strong variability. This holds for a region of intense vertical transport where transport efficiency shows less variability than the sea-to-air flux. On average more source gas particles are entrained than product gas particles. The ratio of SGI and PGI is 1.2 on average and shows some variability ranging from 0.5 to 2. Note that the ratio is calculated for SGI and PGI in mol and that one particle of the source gas CHBr_3 results in three particles of product gas. Therefore although SGI and PGI show similar size when compared in mol the relative importance of SGI is 3.6 times larger than the one of PGI.

In order to determine the potential impact of CHBr_3 and CH_2Br_2 on stratospheric ozone, the ODP, a measure of a substance's destructive effects to the ozone layer relative to the reference substance CFC-11 has been estimated. The ODPs (Fig. 3d) are considerably larger than estimates obtained from previous global model studies

Bromocarbon oceanic emissions and upper air concentrations

S. Tegtmeier et al.

Title Page

Abstract

Introduction

Conclusions

References

Tables

Figures

⏪

⏩

◀

▶

Back

Close

Full Screen / Esc

Printer-friendly Version

Interactive Discussion

(Brioude et al., 2010; Wuebbles et al., 2011). While in these studies mean ODP values were obtained as averages over longer time periods and large regions, we present the first pointwise ODPs calculated individually for emission measurements. ODPs are a function of chemical and transport properties relevant for the VSLS but do not take into account the strength of the emission. As a result the relative ozone-destroying capabilities for VSLS (expressed as ODPs) can be large when transport from the boundary into the stratosphere is efficient while the actual contribution of VSLS to the stratospheric Br_y loading is small due to weak VSLS emissions. In general our estimated ODPs show a large variability where episodic injections estimated for a highly convective region can be orders of magnitude higher than the global mean. However, cases of maximum ODP (or maximum vertical transport) do not coincide with peak emissions of VSLS. Our results indicate that mean ODP values for VSLS obtained by coarse global models mask a large variance over space and time. This can lead to an inaccurate estimation of the VSLS contribution to stratospheric ozone depletion.

3.3 Comparison with SGI and PGI based on tropical Atlantic emissions

It is of interest to compare VSLS emissions and their subsequent atmospheric transport for different oceanic regions. Therefore observations of VSLS emissions during the R/V *Meteor* cruise #55 in the tropical Atlantic in October/November 2002 (Quack et al., 2004) are used to calculate SGI and PGI for CHBr_3 . Figure 4 shows the mean emission for CHBr_3 observed during the *Meteor* #55 and *Sonne TransBrom* cruises. Emissions during both campaigns are on average of very similar magnitude and in the middle range of global mean emission estimates. The sea-to-air flux observed during the *Meteor* #55 cruise is strongly localized (Quack et al., 2004) as it is also the case for *TransBrom*, and includes intense emissions in tropical open ocean regions. Additionally, mean CH_2Br_2 emissions for the *Sonne TransBrom* cruise are displayed which are quite low compared to global mean estimates and compared to CHBr_3 emissions during the same cruise. (Note, that CH_2Br_2 sea-to-air fluxes were not observed during the *Meteor* cruise #55.) For all three cases mean SGI and PGI values are shown

Bromocarbon oceanic emissions and upper air concentrations

S. Tegtmeier et al.

Title Page

Abstract

Introduction

Conclusions

References

Tables

Figures

⏪

⏩

◀

▶

Back

Close

Full Screen / Esc

Printer-friendly Version

Interactive Discussion



in Fig. 4. SGI estimated for CHBr_3 emissions in the tropical Atlantic is relatively low with 1.1 % of all emitted source gases being transported into the tropical stratosphere while in the western Pacific 3.8 % of all emitted source gases are entrained. This difference results from the stronger convective activity in the western Pacific which acts as the main mechanism for the fast vertical uplift of air masses. For PGI similar results are found with stronger entrainment for western Pacific emissions compared to tropical Atlantic emissions. However, for PGI the difference is less pronounced than for SGI indicating that although variability of vertical transport leads to a more efficient SGI and PGI in the western Pacific in the first place, the variability of wet deposition acts to reduce this difference and decreases the PGI more in the western Pacific than in the tropical Atlantic. Overall, the main difference between CHBr_3 entrainment in the western Pacific and in the tropical Atlantic results from differences in the efficiency of the vertical transport from the boundary layer in the emission region into the stratosphere. However, variability of PGI and SGI within one campaign comes mainly from the variability of the emission strength and only in the second place from the variability of the vertical transport (not shown here). For CH_2Br_2 SGI is quite efficient and more than 10 % of the emitted SG are injected into the stratosphere. However, PGI is very low as already discussed for the time series displayed in Fig. 3.

3.4 PG and SG profiles

Based on observed VLSL emissions in the western Pacific and subsequent modeling of atmospheric transport we estimate VLSL vertical profiles in the TTL. In Fig. 5 our emission-based estimates are compared to atmospheric VLSL profiles based on globally available upper air measurements (Montzka and Reimann et al., 2011). This comparison provides a new aspect to the current state of VLSL modeling where an agreement between upper air measurements and model results is obtained by adjusting oceanic emission scenarios instead of using the emission rates as an independent source of information. The emission-based atmospheric VLSL profiles depend on the accurate representation of vertical transport within the model simulation. The

Bromocarbon oceanic emissions and upper air concentrations

S. Tegtmeier et al.

Title Page

Abstract

Introduction

Conclusions

References

Tables

Figures



Back

Close

Full Screen / Esc

Printer-friendly Version

Interactive Discussion



profiles are estimated based on the emission and transport properties of the western Pacific region and do not take into account mixing with air masses from other regions. The measurement-based atmospheric VLSL profiles are estimated from available aircraft and balloon campaigns (Montzka and Reimann et al., 2011) and depend on their observational coverage. Emission-based and measurement-based profiles are not coincident in time and space and can therefore only be compared in a qualitative way. For CHBr_3 emission-based estimates and observations show a good agreement (Fig. 5a). The fact that the relative fraction of upper-air CHBr_3 resulting from western Pacific emission and transport properties is in good agreement with measurement-based global profiles is consistent with the western Pacific emissions being in the middle range of global emission estimates. The mean profiles are of similar magnitude above 15 km with observations being slightly larger. The maximum CHBr_3 abundances derived from observations (0.31 ppt at 17 km) are slightly smaller than the ones derived from the emission-based estimates (0.36 ppt at 17 km) indicating that localized strong sources found at the ocean surface can lead to higher mixing ratios in the upper atmosphere than observed so far. On average CHBr_3 emitted in the western Pacific can lead to atmospheric abundances of 0.07 ppt CHBr_3 at 17 km if not mixed with other air masses. This is smaller than global estimates derived from modeling studies which range between 0.1 ppt and 0.15 ppt (Warwick et al., 2006; Aschmann et al., 2009; Hosaini et al., 2010). For CH_2Br_2 , the emission-based estimates are much smaller than the atmospheric observations (Fig. 5b). This difference is very likely caused by the low emissions observed in the western Pacific during TransBrom, indicating that emissions from other oceanic regions are more important for the stratospheric budget. Also shown are CHBr_3 estimates based on emissions in the tropical Atlantic observed during the Meteor #55 campaign (Fig. 5c). As opposed to the western Pacific estimates the modeled CHBr_3 abundances are considerably smaller than the observed ones. The modeled CHBr_3 drops down to zero above 15 km indicating that there is only very little convectively driven transport reaching the upper TTL on short timescales. Figure 5d shows total Br profiles summarizing VLSL transport calculations for emissions from the

**Bromocarbon
oceanic emissions
and upper air
concentrations**

S. Tegtmeier et al.

Title Page

Abstract

Introduction

Conclusions

References

Tables

Figures



Back

Close

Full Screen / Esc

Printer-friendly Version

Interactive Discussion



western Pacific. Total Br is derived from source gas and product gas abundances individually for CHBr_3 and CH_2Br_2 . Estimates of total Br amount to 0.26 ppt for CHBr_3 (with 80 % from SGI and 20 % from PGI) and 0.12 ppt for CH_2Br_2 (with more than 90 % from SGI). The contribution of both VSLs to stratospheric Br_y is about 0.38 ppt on average (with approximately 80 % from SGI). The major fraction of total Br results from CHBr_3 and its degradation products and only a small part originates from CH_2Br_2 . This relatively low importance of CH_2Br_2 results from the low emissions observed in the western Pacific in October 2009 and can be quite different for other oceanic regions. Globally the contribution of CH_2Br_2 to stratospheric Br_y is expected to be of equal or greater importance compared to CHBr_3 .

4 Summary

The strength and novelty of our study results from modeling upper air VSLs abundances based on observations of highly localized oceanic emissions. SGI and PGI estimated from local sea-to-air flux observations are characterized by a large variability where episodic injections can be orders of magnitude higher than the global mean. Our results indicate that mean values of VSLs SGI and PGI obtained by coarse global models mask a large variance over space and time. This can lead to an inaccurate estimation of the VSLs contribution to stratospheric ozone depletion. Especially if the intensity of vertical transport and the VSLs sea-to air flux are correlated coarse models could potentially over- or underestimate upper air VSLs abundances. Such a correlation has not been observed for above presented emission and transport in the western Pacific since for both bromocarbons, the peak emissions have been determined by strong localized oceanic sources which are not related to atmospheric transport characteristics. However, in a scenario of relatively uniform oceanic concentrations the emission rates could be determined by the wind speed variations which would enable a correlation between emission strength and vertical transport intensity.

CHBr_3 and CH_2Br_2 emitted in the western Pacific, a region of intense vertical trans-

Bromocarbon oceanic emissions and upper air concentrations

S. Tegtmeier et al.

Title Page

Abstract

Introduction

Conclusions

References

Tables

Figures



Back

Close

Full Screen / Esc

Printer-friendly Version

Interactive Discussion



**Bromocarbon
oceanic emissions
and upper air
concentrations**

S. Tegtmeier et al.

Title Page

Abstract

Introduction

Conclusions

References

Tables

Figures



Back

Close

Full Screen / Esc

Printer-friendly Version

Interactive Discussion

port, have a large potential to destroy stratospheric ozone as illustrated by their high ODP values. Where and when strong vertical transport and strong emissions coincide, large VSLS entrainment into the stratosphere can be expected. For CHBr_3 mean emission-based estimates are consistent with upper air observations while peak emissions lead to larger than so far observed atmospheric abundances. Our results show the importance of the western Pacific as a VSLS entrainment region and illustrate the need for quantifying the spatial and temporal variability of CHBr_3 emission rates. For CH_2Br_2 observed emission in the western Pacific and estimated atmospheric abundances are considerably lower than observations. Both bromocarbons will contribute directly and in form of their product gases to the stratospheric bromine loading. Current observational estimates of the total contribution of all VSLS to the stratospheric bromine budget range around 5 pptv. Our emission-based estimates of CHBr_3 and CH_2Br_2 yield a direct source gas contribution of the two bromocarbons to the stratospheric bromine loading of 0.3 pptv Br on average and 1.7 pptv Br in a maximum case. Together with PGI this results in a total Br entrainment of 0.4 pptv on average and 2.3 pptv for cases of maximum emissions.

Acknowledgements. We thank the TransBrom Sonne team for collecting the VSLS measurements. The authors would also like to thank the group of Elliot Atlas for analysing and providing the atmospheric VSLS surface concentrations. The authors are grateful to the ECMWF for making the reanalysis product ERA-Interim available. This study is carried out within the WGL-project TransBrom.

References

- Aschmann, J., Sinnhuber, B.-M., Atlas, E. L., and Schauffler, S. M.: Modeling the transport of very short-lived substances into the tropical upper troposphere and lower stratosphere, *Atmos. Chem. Phys.*, 9, 9237–9247, doi:10.5194/acp-9-9237-2009, 2009.
- Brioude, J., Portmann, R. W., Daniel, J. S., Cooper, O. R., Frost, G. J., Rosenlof, K. H., Granier, C., Ravishankara, A. R., Montzka, S. A., and Stohl, A.: Variations in ozone depletion poten-

**Bromocarbon
oceanic emissions
and upper air
concentrations**

S. Tegtmeier et al.

[Title Page](#)[Abstract](#)[Introduction](#)[Conclusions](#)[References](#)[Tables](#)[Figures](#)[⏪](#)[⏩](#)[◀](#)[▶](#)[Back](#)[Close](#)[Full Screen / Esc](#)[Printer-friendly Version](#)[Interactive Discussion](#)

tials of very short-lived substances with season and emission region. *Geophys. Res. Lett.*, 37, L19804, doi:10.1029/2010GL044856, 2010.

Butler, J. H., King, D. B., Lobert, J. M., Montzka, S. A., Yvon-Lewis, S. A., Hall, B. D., Warwick, N. J., Mondeel, D. J., Aydin, M., and Elkins, J. W.: Oceanic distributions and emissions of short-lived halocarbons, *Global Biogeochem. Cy.*, 21, GB1023, doi:10.1029/2006GB002732, 2007.

Carpenter, L. J. and Liss, P. S.: On temperate sources of Bromoform and other reactive organic bromine gases, *J. Geophys. Res.* 105, 20539–20547, 2000.

Dee, D. P., Uppala, S. M., Simmons, A. J., Berrisford, P., Poli, P., Kobayashi, S., Andrae, U., Balmaseda, M. A., Balsamo, G., Bauer, P., Bechtold, P., Beljaars, A. C. M., van de Berg, L., Bidlot, J., Bormann, N., Delsol, C., Dragani, R., Fuentes, M., Geer, A. J., Haimberger, L., Healy, S. B., Hersbach, H., Hólm, E. V., Isaksen, L., Kållberg, P., Köhler, M., Matricardi, M., McNally, A. P., Monge-Sanz, B. M., Morcrette, J.-J., Park, B.-K., Peubey, C., de Rosnay, P., Tavolato, C., Thépaut, J.-N., and Vitart, F.: The ERA-Interim reanalysis: configuration and performance of the data assimilation system, *Q. J. Roy. Meteor. Soc.*, 137, 553–597, 2011.

Dorf, M., Butz, A., Camy-Peyret, C., Chipperfield, M. P., Kritten, L., and Pfeilsticker, K.: Bromine in the tropical troposphere and stratosphere as derived from balloon-borne BrO observations, *Atmos. Chem. Phys.*, 8, 7265–7271, doi:10.5194/acp-8-7265-2008, 2008.

Forster, C., Wandinger, U., Wotawa, G., James, P., Mattis, I., Althausen, D., Simmonds, P., O'Doherty, S., Kleefeld, C., Jennings, S. G., Schneider, J., Trickl, T., Kreipl, S., Jäger, H., and Stohl, A.: Transport of boreal forest fire emissions from Canada to Europe, *J. Geophys. Res.*, 106, 22887–22906, 2001.

Forster, C., Cooper, O., Stohl, A., Eckhardt, S., James, P., Dunlea, E., Nicks, D. K., Holloway, Jr. J. S., Hübler, G., Parrish, D. D., Ryerson, T. B., and Trainer, M.: Lagrangian transport model forecasts and a transport climatology for the Intercontinental Transport and Chemical Transformation 2002 (ITCT 2k2) measurement campaign, *J. Geophys. Res.*, 109, D07S92, doi:10.1029/2003JD003589, 2004.

Forster, C., Stohl, A., and Seibert, S.: Parameterization of Convective Transport in a Lagrangian Particle Dispersion Model and Its Evaluation, *J. Appl. Meteor. Climatol.*, 46, 403–422, 2007.

Garcia, R. R. and Solomon, S.: A new numerical model of the middle atmosphere: 2. Ozone and related species, *J. Geophys. Res.*, 99, 12937–12951, doi:10.1029/94JD00725, 1994.

Gettelman, A., Lauritzen, P. H., Park, M., and Kay, J. E.: Processes regulating short-lived species in the tropical tropopause layer, *J. Geophys. Res.*, 114, D13303,

**Bromocarbon
oceanic emissions
and upper air
concentrations**

S. Tegtmeier et al.

Title Page

Abstract

Introduction

Conclusions

References

Tables

Figures

⏪

⏩

◀

▶

Back

Close

Full Screen / Esc

Printer-friendly Version

Interactive Discussion

doi:10.1029/2009JD011785, 2009.

Hossaini, R., Chipperfield, M. P., Monge-Sanz, B. M., Richards, N. A. D., Atlas, E., and Blake, D. R.: Bromoform and dibromomethane in the tropics: a 3-D model study of chemistry and transport, *Atmos. Chem. Phys.*, 10, 719–735, doi:10.5194/acp-10-719-2010, 2010.

5 Kerkweg, A., Jöckel, P., Warwick, N., Gebhardt, S., Brenninkmeijer, C. A. M., and Lelieveld, J.: Consistent simulation of bromine chemistry from the marine boundary layer to the stratosphere – Part 2: Bromocarbons, *Atmos. Chem. Phys.*, 8, 5919–5939, doi:10.5194/acp-8-5919-2008, 2008.

Ko, M. K. W., Poulet, G., Blake, D. R., et al.: Very short-lived halogen and sulfur substances, Scientific assessment of ozone depletion: 2002, Global Ozone Research and Monitoring Project – Report No. 47, Chapter 2, Geneva, Switzerland, 2003.

10 Krüger, K. and Quack, B.: Introduction to special issue: the TransBrom Sonne expedition in the tropical West Pacific, *Atmos. Chem. Phys. Discuss.*, 12, 1401–1418, doi:10.5194/acpd-12-1401-2012, 2012.

15 Laube, J. C., Engel, A., Bönisch, H., Möbius, T., Worton, D. R., Sturges, W. T., Grunow, K., and Schmidt, U.: Contribution of very short-lived organic substances to stratospheric chlorine and bromine in the tropics – a case study, *Atmos. Chem. Phys.*, 8, 7325–7334, doi:10.5194/acp-8-7325-2008, 2008.

20 Law, K. S., Sturges, W. T., Blake, D. R., et al.: Halogenated very short-lived substances, Scientific Assessment of Ozone Depletion: 2006, Global Ozone Research and Monitoring Project – Report No. 50, Geneva, Switzerland, 2007.

Liang, Q., Stolarski, R. S., Kawa, S. R., Nielsen, J. E., Douglass, A. R., Rodriguez, J. M., Blake, D. R., Atlas, E. L., and Ott, L. E.: Finding the missing stratospheric Br_y: a global modeling study of CHBr₃ and CH₂Br₂, *Atmos. Chem. Phys.*, 10, 2269–2286, doi:10.5194/acp-10-2269-2010, 2010.

25 Livesey, N. J., Kovalenko, L. J., Salawitch, R., J., MacKenzie, I. A., Chipperfield, M. P., Read, W. G., Jarnot, R. F., and Waters, J. W.: EOS Microwave Limb Sounder observations of upper stratospheric BrO: Implications for bromine, *Geophys. Res. Lett.*, 33, L20817, doi:10.1029/2006GL026930, 2006.

30 McElroy, M. B., Salawich, R. J., Wofsy, S. C., and Logan, J. A.: Reductions of Antarctic ozone due to synergistic interactions of chlorine and bromine, *Nature*, 321, 759–762, 1986.

McLinden, C. A., Haley, C. S., Lloyd, N. D., Hendrick, F., Rozanov, A., Sinnhuber, B.-M., Goutail, F., Degenstein, D. A., Llewellyn, E. J., Sioris, C. E., Van Roozendaal, M., Pom-

**Bromocarbon
oceanic emissions
and upper air
concentrations**

S. Tegtmeier et al.

[Title Page](#)[Abstract](#)[Introduction](#)[Conclusions](#)[References](#)[Tables](#)[Figures](#)[⏪](#)[⏩](#)[◀](#)[▶](#)[Back](#)[Close](#)[Full Screen / Esc](#)[Printer-friendly Version](#)[Interactive Discussion](#)

mereau, J. P., Lotz, W., and Burrows, J. P.: Odin/OSIRIS observations of stratospheric BrO: Retrieval methodology, climatology, and inferred Bry, *J. Geophys. Res.*, 115, D15308, doi:10.1029/2009JD012488, 2010.

Montzka, S. A., Reimann, S., et al.: Ozone-depleting substances and related chemicals, Scientific Assessment of Ozone Depletion: 2010, Global Ozone Research and Monitoring Project – Report No. 52, Geneva, Switzerland, 2011.

Nightingale, P. D., Malin, G., Law, C. S., Watson, A. J., Liss, P. S., Liddicoat, M. I., Boutin, J., and Upstill-Goddard, R. C.: In situ evaluation of airsea gas exchange parameterizations using novel conservative and volatile tracers, *Global Biogeochem. Cy.*, 14, 373–387, 2000.

Pisso, I., Haynes, P. H., and Law, K. S.: Emission location dependent ozone depletion potentials for very short-lived halogenated species, *Atmos. Chem. Phys.* 10, 12025–12036, doi:10.5194/acp-10-12025-2010, 2010.

Quack, B. and Wallace, D. W. R.: Air-sea flux of bromoform: Controls, rates and implications, *Global Biogeochem. Cy.* 17, 1023, doi:10.1029/2002GB001890, 2003.

Quack, B., Atlas, E., Petrick, G., Stroud, V., Schauffler, S., and Wallace, D. W. R.: Oceanic bromoform sources for the tropical atmosphere, *Geophys. Res. Lett.*, 31, L23S05, doi:10.1029/2004GL020597, 2004.

Quack, B., Atlas, E., Petrick, G., and Wallace, D. W. R.: Bromoform and dibromomethane above the Mauritanian upwelling: Atmospheric distributions and oceanic emissions, *J. Geophys. Res.*, 112, D09312, doi:10.1029/2006JD007614, 2007.

Salawitch, R. J., Weisenstein, D. K., Kovalenko, L. J., Sioris, C. E., Wennberg, P. O., Chance, K., Ko, M. K. W., and McLinden, C. A.: Sensitivity of ozone to bromine in the lower stratosphere, *Geophys. Res. Lett.*, 32, L05811, doi:10.1029/2004GL021504, 2005.

Schauffler, S. M., Atlas, E. L., Flocke, F., Lueb, R. A., Stroud, V., and Travnicek, W.: Measurements of bromine containing organic compounds at the tropical tropopause, *Geophys. Res. Lett.*, 25, 317–320, 1998.

Schauffler, S. M., Atlas, E. L., Blake, D. R., Flocke, F., Lueb, R. A., Lee-Taylor, J. M., Stroud, V., and Travnicek, W.: Distributions of brominated organic compounds in the troposphere and lower stratosphere, *J. Geophys. Res.*, 104, 21513–21535, 1999.

Sinnhuber, B.-M., Arlander, D. W., Bovensmann, H., Burrows, J. P., Chipperfield, M. P., Enell, C.-F., Frieß, U., Hendrick, F., Johnston, P. V., Jones, R. L., Kreher, K., Mohamed-Tahrin, N., Müller, R., Pfeilsticker, K., Platt, U., Pommereau, J.-P., Pundt, I., Richter, A., South, A. M., Tørnkvist, K. K., Van Roozendaal, M., Wagner, T., and Wittrock, F.: Comparison of

Bromocarbon oceanic emissions and upper air concentrations

S. Tegtmeier et al.

[Title Page](#)
[Abstract](#)
[Introduction](#)
[Conclusions](#)
[References](#)
[Tables](#)
[Figures](#)
[⏪](#)
[⏩](#)
[◀](#)
[▶](#)
[Back](#)
[Close](#)
[Full Screen / Esc](#)
[Printer-friendly Version](#)
[Interactive Discussion](#)


measurements and model calculations of stratospheric bromine monoxide, *J. Geophys. Res.*, 107, 4398, doi:10.1029/2001JD000940, 2002.

Sinnhuber, B.-M., Rozanov, A., Sheode, N., Afe, O. T., Richter, A., Sinnhuber, M., Wittrock, F., Burrows, J. P., Stiller, G. P., von Clarmann, T., and Linden, A.: Global observations of stratospheric bromine monoxide from SCIAMACHY, *Geophys. Res. Lett.*, 32, L20810, doi:10.1029/2005GL023839, 2005.

Sioris, C. E., Kovalenko, L. J., McLinden, Salawitch, R. J., Van Roozendael, M., Goutail, F., Dorf, M., Pfeilsticker, K., Chance, K., von Savigny, C., Liu, X., Kurosu, T. P., Pomereau, J.-P., Bösch, H., and Frerick, J.: Latitudinal and vertical distribution of bromine monoxide in the lower stratosphere from Scanning Imaging Absorption Spectrometer for Atmospheric Chartography limb scattering measurements, *J. Geophys. Res.*, 111, D14301, doi:10.1029/2005JD006479, 2006.

Solomon, S., Wuebbles, D. J., Isaksen, L., Kiehl, J., Lal, M., Simon, P., and Sze, N.: Ozone depletion potentials, global warming potentials, and future chlorine/bromine loading, Scientific assessment of ozone depletion: 1994, Global Ozone Research and Monitoring Project Report No. 37, World Meteorological Organization, Geneva, Switzerland, 13.1–13.36, 1995.

Spichtinger, N., Wenig, M., James, P., Wagner, T., Platt, U., and Stohl, A.: Satellite detection of a continental-scale plume of nitrogen oxides from boreal forest fires, *Geophys. Res. Lett.*, 28, 4579–4582, 2001.

Stohl, A. and Thomson, D. J.: A density correction for Lagrangian particle dispersion models, *Bound.-Layer Meteorol.*, 90, 155–167, 1999.

Stohl, A. and Trickl, T.: A textbook example of long-range transport: Simultaneous observation of ozone maxima of stratospheric and North American origin in the free troposphere over Europe, *J. Geophys. Res.*, 104, 30445–30462, 1999.

Stohl, A., Hittenberger, M., and Wotawa, G.: Validation of the Lagrangian particle dispersion model FLEXPART against large scale tracer experiment data, *Atmos. Environ.*, 32, 4245–4264, 1998.

Stohl, A., Forster, C., Eckhardt, S., Spichtinger, N., Huntrieser, H., Heland, J., Schlager, H., Wilhelm, S., Arnold, F., and Cooper, O.: A backward modeling study of intercontinental pollution transport using aircraft measurements, *J. Geophys. Res.*, 108, 4370, doi:10.1029/2002JD002862, 2003.

Stohl, A., Forster, C., Frank, A., Seibert, P., and Wotawa, G.: Technical note: The Lagrangian particle dispersion model FLEXPART version 6.2, *Atmos. Chem. Phys.*, 5, 2461–

Bromocarbon oceanic emissions and upper air concentrations

S. Tegtmeier et al.

Title Page

Abstract

Introduction

Conclusions

References

Tables

Figures

⏪

⏩

◀

▶

Back

Close

Full Screen / Esc

Printer-friendly Version

Interactive Discussion

2474, doi:10.5194/acp-5-2461-2005, 2005.

Tokarczyk, R. and Moore, R.: Production of volatile organohalogenes by phytoplankton cultures, *Geophys. Res. Lett.*, 21, 285–288, doi:10.1029/94GL00009, 1994.

von Glasow, R., von Kuhlmann, R., Lawrence, M. G., Platt, U., and Crutzen, P. J.: Impact of reactive bromine chemistry in the troposphere, *Atmos. Chem. Phys.*, 4, 2481–2497, doi:10.5194/acp-4-2481-2004, 2004.

Warwick, N. J., Pyle, J. A., Carver, G. D., Yang, X., Savage, N. H., O'Connor, F. M., and Cox, R. A.: Global modeling of biogenic bromocarbons, *J. Geophys. Res.*, 111, D24305, doi:10.1029/2006JD007264, 2006.

Wuebbles, D. J., Patten, K. O., Wang, D., Youn, D., Martínez-Avilés, M., and Francisco, J. S.: Three-dimensional model evaluation of the Ozone Depletion Potentials for n-propyl bromide, trichloroethylene and perchloroethylene, *Atmos. Chem. Phys.*, 11, 2371–2380, doi:10.5194/acp-11-2371-2011, 2011.

Yang, X., Cox, R. A., Warwick, N. J., Pyle, J. A., Carver, G. D., O'Connor, F. M., and Savage, N. H.: Tropospheric bromine chemistry and its impacts on ozone: A model study, *J. Geophys. Res.*, 110, D23311, doi:10.1029/2005JD006244, 2005.

Yang, X., Pyle, J. A., Cox, R. A., Theys, N., and Van Roozendael, M.: Snow-sourced bromine and its implications for polar tropospheric ozone, *Atmos. Chem. Phys.*, 10, 7763–7773, doi:10.5194/acp-10-7763-2010, 2010.

Yokouchi, Y., Hasebe, F., Fujiwara, M., Takashima, H., Shiotani, M., Nishi, N., Kanaya, Y., Hashimoto, S., Fraser, P., Toom-Sauntry, D., Mukai, H., and Nojiri, Y.: Correlations and emission ratios among bromoform, dibromochloromethane, and dibromomethane in the atmosphere, *J. Geophys. Res.* 110, D23309, doi:10.1029/2005JD006303, 2005.

Bromocarbon oceanic emissions and upper air concentrations

S. Tegtmeier et al.

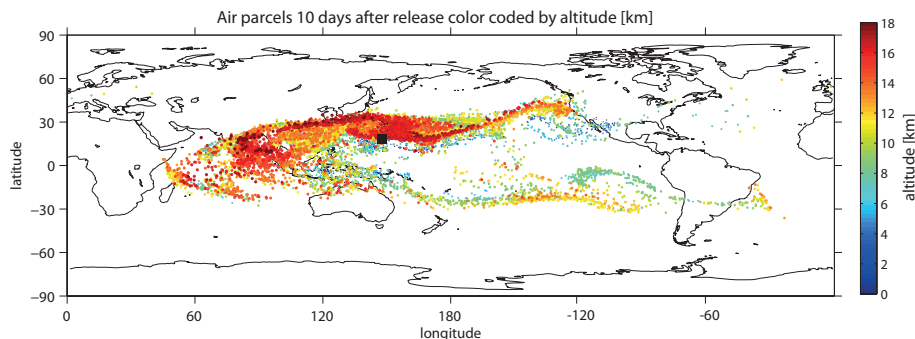


Fig. 1. Spatial distribution on 24 October 2009, of air parcels originally released at the surface at 19° N, 148° E on 14 October 2009, i.e. 10 days after their release. The air parcels are color coded by altitude. Air mass transport including convection has been calculated with the Lagrangian particle dispersion model FLEXPART.

[Title Page](#)[Abstract](#)[Introduction](#)[Conclusions](#)[References](#)[Tables](#)[Figures](#)[◀](#)[▶](#)[◀](#)[▶](#)[Back](#)[Close](#)[Full Screen / Esc](#)[Printer-friendly Version](#)[Interactive Discussion](#)

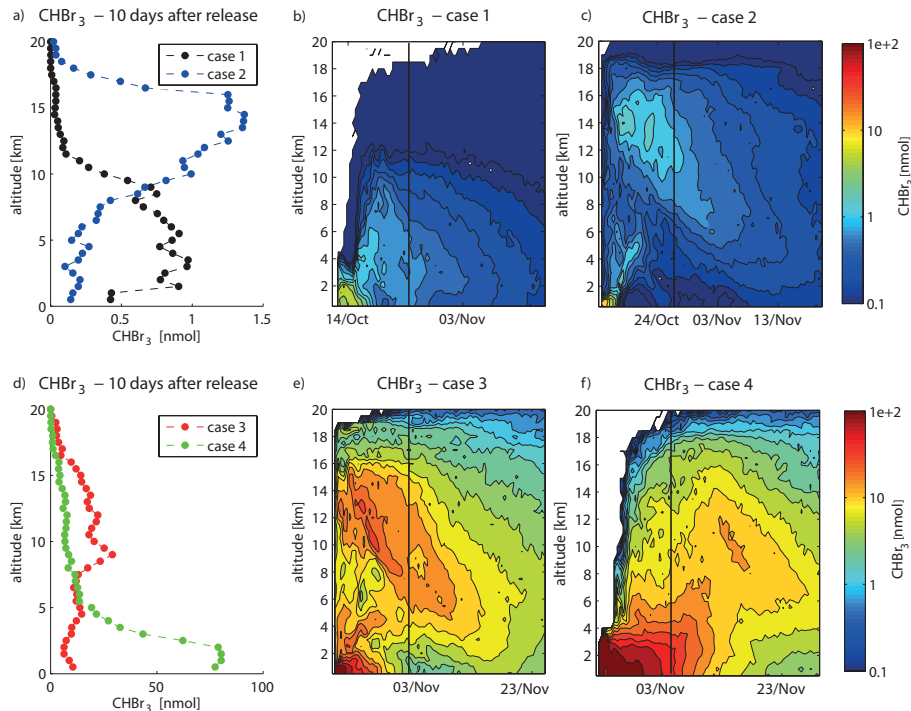


Fig. 2. The vertical distribution of tropical CHBr_3 [nmol] 10 days after the release event is displayed for four case studies (**a** and **d**). Vertical distribution of tropical CHBr_3 over a one month time period starting at the date of the release event is shown (**b**, **c**, **e**, and **f**) with black lines indicating 10 days after the release event. The four case studies are based on observed CHBr_3 sea-to-air fluxes at 30°N , 145°E on 10 October 2009 (case 1), at 19°N , 148°E on 14 October 2009 (case 2), at 3°S , 154°E on 19 October 2009 (case 3), and at 18°S , 145°E on 23 October 2009 (case 4).

Bromocarbon oceanic emissions and upper air concentrations

S. Tegtmeier et al.

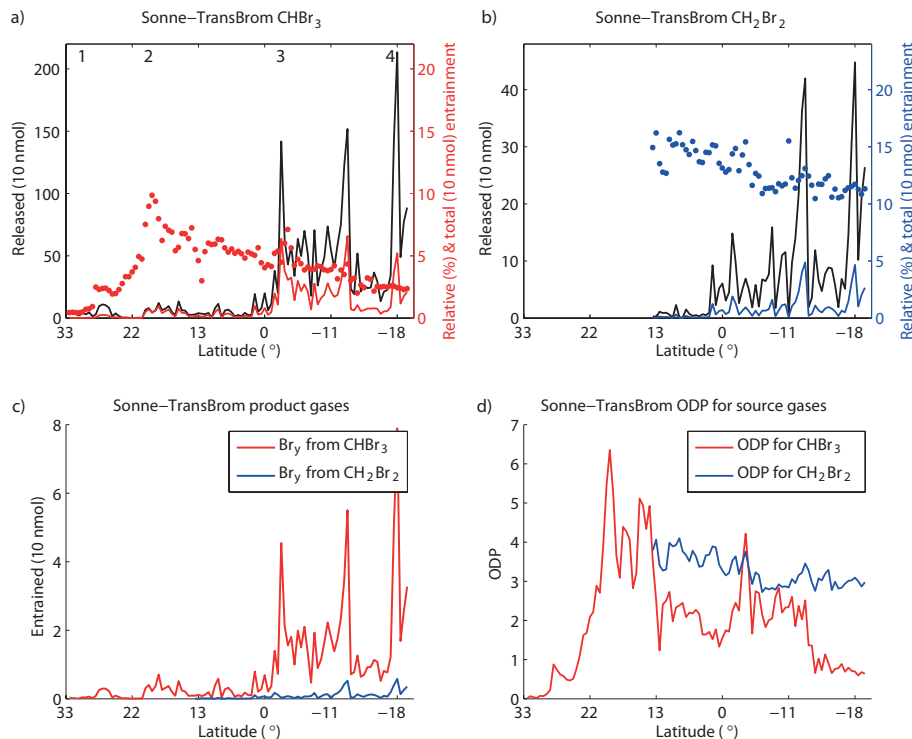


Fig. 3. Observed emissions of VSLs for one hour over 500 m^2 (black line), and relative (colored dots) and total (colored line) amount of VSLs entrained above 17 km for CHBr_3 (a) and CH_2Br_2 (b) are shown. For CHBr_3 the four numbers indicate the four case studies discussed in the text. PGI is given based on CHBr_3 and CH_2Br_2 emissions (c). Ozone depletion potential as a function of emission location is displayed for both VSLs (d).

[Title Page](#)
[Abstract](#)
[Introduction](#)
[Conclusions](#)
[References](#)
[Tables](#)
[Figures](#)
[◀](#)
[▶](#)
[◀](#)
[▶](#)
[Back](#)
[Close](#)
[Full Screen / Esc](#)
[Printer-friendly Version](#)
[Interactive Discussion](#)

**Bromocarbon
oceanic emissions
and upper air
concentrations**

S. Tegtmeier et al.

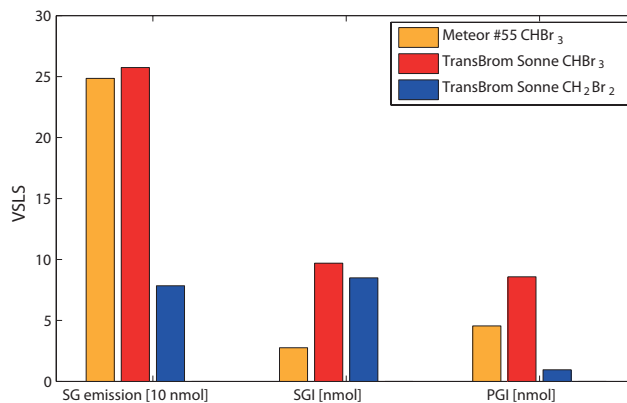


Fig. 4. Average SG emissions of CHBr_3 and CH_2Br_2 observed in the western Pacific during the TransBrom Sonne campaign and in the tropical Atlantic during the Meteor #55 campaign are shown. Total SGI and PGI based on the observed emissions are also displayed.

[Title Page](#)[Abstract](#)[Introduction](#)[Conclusions](#)[References](#)[Tables](#)[Figures](#)[⏪](#)[⏩](#)[◀](#)[▶](#)[Back](#)[Close](#)[Full Screen / Esc](#)[Printer-friendly Version](#)[Interactive Discussion](#)

Bromocarbon oceanic emissions and upper air concentrations

S. Tegtmeier et al.

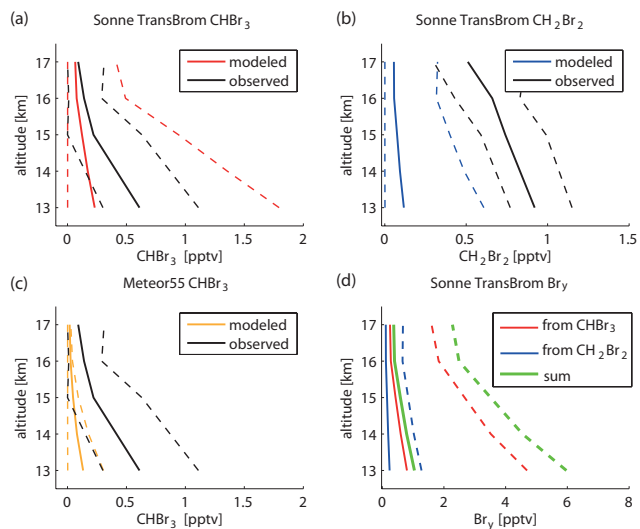


Fig. 5. VLSL profiles based on atmospheric observations (black lines) and estimated from observed emissions (colored lines) of western Pacific CHBr₃ **(a)**, western Pacific CH₂Br₂ **(b)**, and tropical Atlantic CHBr₃ **(c)** are shown. Also total Br profiles (PG and SG) based on western Pacific CHBr₃ and CH₂Br₂ emissions are displayed **(d)**. For all profiles lower and upper limits (dashed lines) and mean values (solid lines) are given.

Title Page

Abstract

Introduction

Conclusions

References

Tables

Figures

◀

▶

◀

▶

Back

Close

Full Screen / Esc

Printer-friendly Version

Interactive Discussion